Fabrication and Evaluation of Graphene Oxide-Titania Nanosheet Composite Membrane for Enhanced Ion Sieving

Hongfan Deng

Received June 10, 2024
Accepted November 20, 2024
Electronic access December 31, 2024

The growing scarcity of freshwater resources has intensified the need for efficient desalination technologies. In recent years, graphene oxide (GO) and titania have emerged as highly promising candidates for membrane fabrication, owing to their exceptional physicochemical properties. In this study, we present a comprehensive investigation into the synthesis, characterization, and application of two-dimensional GO-titania nanosheet composite membranes for ion sieving. Firstly, layered potassium lithium titanate crystals $K_{0.8}Ti_{1.73}Li_{0.27}O_4$ were produced by a solid-state growth method. The crystals were converted into monolayer titania nanosheets (TiNS) through acid-exchange and liquid phase exfoliation. X-ray diffraction (XRD) analysis and characterization techniques such as SEM, TEM and AFM confirmed the presence of monolayer $Ti_{0.87}O_2$ nanosheets in the colloidal solution. Fabrication of GO-TiNS composite membranes was achieved by employing vacuum filtration of a well-dispersed mixture containing GO nanosheets and TiNS. Ion selectivity of the membranes was evaluated for their ion sieving capabilities. Results showed that the permeation rates of Mg^{2+} decreased faster than that of Li^+ with addition of TiNS, and the Li^+/Mg^{2+} separation ratio is 1.08, 1.65, 1.87, 1.83 for GO, GO-TiMS1.2, GO-TiNS2.0 and GO-TiNS2.5 membrane, respectively. The best selectivity for Li^+/Mg^{2+} was achieved with 2.0% of TiNS in GO. Our results indicate TiNS could increase the separation capability of GO membrane between Li^+ and Mg^{2+}. This work demonstrates the potential of GO and TiNS for future application in the design and optimization of advanced ion-selective membranes.

Keywords: Graphene oxide; Titania nanosheets; Nanocomposite membranes; Ion sieving; Li^+/Mg^{2+} selectivity

Introduction

Separation is one of the significant technologies for monitoring anthropogenic pollutants in aquatic systems and enhancing efficiencies of various types of batteries, contributing to enormous economic effects, clean energy generation, and a sustainable ecosystem[1]. Traditional separation methods include absorption[2], extractive distillation[3], crystallization[4], etc. These approaches have been broadly applied in industrial processes but take up 10-15% of energy consumption in the world and 50% of that in the chemical industry. Among novel separation technologies, ion-selective membranes have garnered immense attention in recent years, owing to their pivotal role in various applications such as desalination, energy storage, and separation processes[5]. These membranes are engineered to allow selective transport of ions while impeding the passage of other species, facilitating the efficient separation and purification of diverse ionic species. Membranes prepared from two-dimensional (2D) materials have demonstrated remarkable properties, such as exceptional selectivity, high permeability, and enhanced durability, making them promising candidates for water purification or resource recycling[6]. Among common types of ion-sieving membranes, reverse osmosis membranes, nanofiltration membranes, and electrodialysis membranes mainly employ polymeric composite materials, while other membranes also use graphene/graphene oxide, zeolites, or other materials. Various composite materials are fabricated into membranes to improve ion selectivity via size exclusion, electric charge interaction and co-enhancement of size exclusion and electric charge interaction, allowing certain ionic species to be selected and therefore leading to different applications[7].

Graphene oxide (GO), a derivative of graphene, possesses a 2D structure with oxygen-containing functional groups. This structure imparts remarkable mechanical strength, high surface area, and excellent chemical stability to graphene oxide[8]. However, the natural tendency of GO laminates to swell in water can significantly reduce its separation performance[9]. Numerous studies have been done to modulate the interlayer spacing of GO membranes, such as chemical reduction, cation controlling, and building multilayer architectures[10]. In addition, exfoliation of micro-sized 2D materials into nanosheets is essential for constructing layered membranes. Titania nanosheets (TiNS), as a 2D nanomaterial with high crystallinity and exceptionally low thickness, have been heavily investigated for the superior photocatalytic activity, chemical stability, and ion adsorption capacity of titania[11]. Previous study has reported the synthesis of TiNS

by exfoliating protonic titanate crystals [12]. The electronegativity of TiNS can cause negatively charged graphene nanosheets to align through electrostatic repulsion during the membrane assembly. High-quality graphene hybrid films were fabricated by adding a small quantity of TiNS and exhibited significantly improved mechanical flexibility and electrical properties [13]. Hybrid films of graphene oxide (GO) and monolayer titania (TO) were assembled and demonstrated tunable hydrophilicity [14]. Therefore, the combination of the GO and TiNS may exhibit a unique property that make them ideal candidates for ion sieving.

In this study, we fabricated highly aligned 2D GO-TiNS composite membranes by adding a small quantity of TiNS. The high electronegativity of TiNS enhances the electrostatic interactions with GO nanosheets, which promotes better arrangement of the GO nanosheets. The resulting GO-TiNS composite membrane show enhanced ion sieving properties. Our work demonstrates the potential of GO and TiNS for future application in the design and optimization of advanced ion-selective membranes.

Results

Characterizations of fabricated composite

By employing a high-temperature solid-state growth method, we generated plate-like $K_{0.8}Ti_{1.73}Li_{0.27}O_4$ microcrystals with an average lateral dimension ranging from 2 to 3 μm, as depicted in Figure 1a through SEM imaging. Following an acid leaching process, the material transformed to the protonated form ($H_{1.07}Ti_{1.73}O_4$), resulting in some degree of loosening in the plate crystals (Figure 1b).

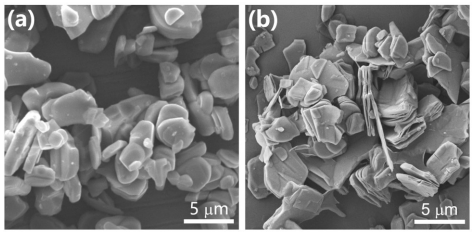

Fig. 1 SEM images of (a) layered $K_{0.8}Ti_{1.73}Li_{0.27}O_4$ crystals and (b) protonated titania $H_{1.07}Ti_{1.73}O_4$ crystals.

The XRD patterns of layered and protonated crystals are shown in Figure 2. By comparing the diffraction peaks with a standard card library, the phase analysis results confirm the presence of $H_{1.07}Ti_{1.73}O_4$ in the protonated phase (Figure 2b). There is an absence of the diffraction peak, which is a characteristic of the $K_{0.8}Ti_{1.73}Li_{0.27}O_4$ layered phase (Figure 2a), indicating a complete exchange of interlayer K^+ ions with H^+ ions. Notably, the most prominent peak in the protonated phase corresponds to the diffraction peak at $2\theta = 9.61^\circ$, indicating an expanded interlayer distance of $d = 0.92$nm. In contrast, the interlayer distance of layered crystals is 0.77nm, highlighting the substantial increase in interlayer spacing in the protonated phase.

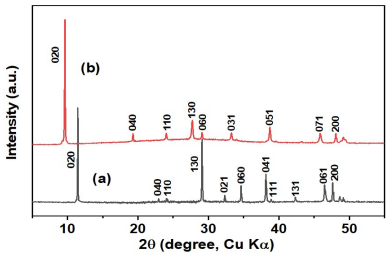

Fig. 2 XRD patterns of (a) layered $K_{0.8}Ti_{1.73}Li_{0.27}O_4$ crystals and (b) protonated titania $H_{1.07}Ti_{1.73}O_4$ crystals.

Then the protonic titanate crystals were reacted with an aqueous tetramethylammonium hydroxide (TMBOH) solution, resulting in the intercalation of TMB^+ ions along with H_2O molecules. The layered titanate crystals were exfoliated into molecular nanosheets TiNS. The suspension exhibited a lustrous texture (Figure 3a), indicating the presence of quasi-long-range molecular organization and the formation of a nematic liquid crystalline mesophase. The obtained TiNS were examined by TEM and AFM observations. As shown in the TEM image (Figure 3b), the lateral sizes of TiNS were in the range of 1$\sim$2 μm. Atomic force microscope (AFM) analysis confirmed that the substance in the colloidal solution consisted monolayer sheets, measuring approximately 2.3 nm in thickness (Figure 3c, 3d).

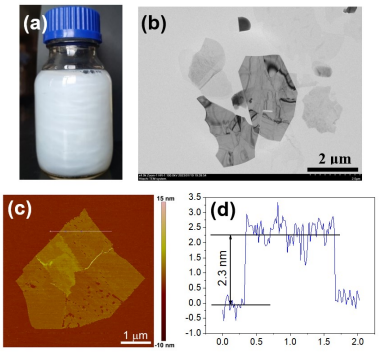

Fig. 3 Characteristics of titanate nanosheets TiNS. (a) Picture of the exfoliated TiNS colloidal solution showing a lustrous texture. (b) TEM image of TiNS. (c) AFM image of TiNS deposited on a mica substrate. (d) The height profile of TiNS along the white line marked in the AFM image.

The GO-TiNS composite membranes were fabricated by vacuum filtration of a homogeneously dispersed mixture of GO nanosheets and TiNS. By changing the mass fraction x wt% of TiNS, the obtained composite membranes were denoted as GO-TiNSx. Membrane GO-TiNS1.2 was used for membrane characterization compared with pristine GO membrane.

The morphological features of composite membranes were investigated. Compared with the dark black of GO membrane,

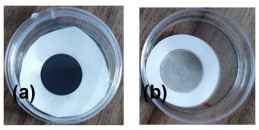

Fig. 4 Photographs of (a) GO and (b) GO-TiNS1.2 membranes.

the composite membranes exhibited light black (Figure 4). Top-view SEM observation demonstrated some degree of corrugation on the GO membrane surface (Figure 5a), which may exert notable effects on their chemical reactivity and electrochemical properties [15]. This corrugation was mitigated with incorporation of titania nanosheets (Figure 5b). These changes in appearance implied a difference in inner structure and compositional characteristics of the membranes. Cross-sectional SEM observation clearly demonstrates the lamellar structures of GO-TiNS membrane (Figure 5c,d).

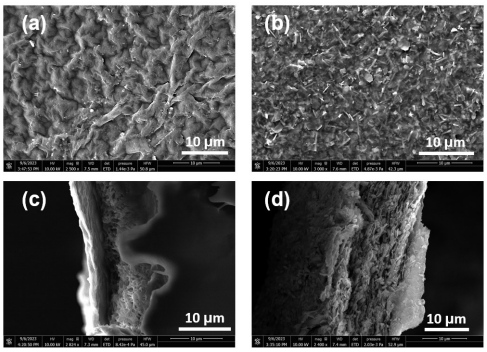

Fig. 5 Surface SEM images of (a) GO and (b) GO-TiNS2.0 membranes. Cross-sectional SEM images of (c) GO and (d) GO-TiNS2.0 membranes.

The membrane surfaces were further examined by in situ attenuated total reflection Fourier-transform infrared spectroscopy (ATR-FTIR). FTIR is commonly used to characterize chemical composition by measuring the absorbance of light through a sample as a function of wavelength to identify the chemical bonds and functional groups in a composite [16]. ATR-FTIR is a label-free, non-destructive analytical method to obtain IR spectra with an internal reflection element and commonly used for membrane characterization [17]. Figure 6 presents the FTIR spectra of GO and GO-TiNS composite membranes in the wavenumber range of 500-4000 cm^{-1}. The FTIR spectrum for GO membrane shows a large number of functional groups. For both membranes, the broad band between 3600-3000 cm^{-1} can be assigned to stretching vibration of hydroxyl (OH) [18]. The peak at 1724 cm^{-1} and 1631 cm^{-1} can be attributed to C=O stretching of carbonyl group. The absorption peaks at 1600-1400 cm^{-1} can be assigned to the C=C of graphene [19]. In the case of GO-TiNS composite membrane, the intense peak at 938 can be attributed to Ti-O stretching which is the characteristic of the formation of Ti-O-Ti network [20], while the FTIR spectrum also keeps some features of GO components [21]. The above results indicate highly aligned hybrid membranes were obtained.

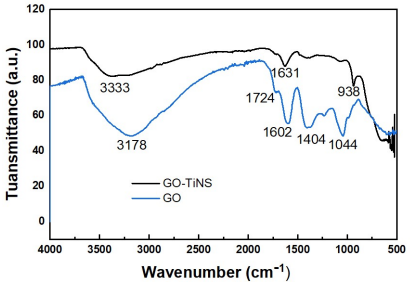

Fig. 6 ATR-FTIR spectra of GO and GO-TiNS1.2 membranes.

The effects of TiNS on membrane separation performance

To investigate the transmembrane properties of ions, the membrane was clamped in an ion permeation device. The conductivity of a solution is proportional to the number of ions, therefore, can be used to determine the salt concentration using a series of known standard solutions. The conductivity of the salt solution in the raw side was measured every 10 min for 1 h. The salt concentrations in the raw side at each time point were obtained. As shown in Figure 7a, the ion concentrations in the raw side increased linearly with time. As Li^+ has smaller hydration diameter [22], its permeation rate was higher than that of Mg^{2+} for both GO and GO-TiNS membranes. To further investigate the impact of TiNS amendment on ion selectivity of the membranes, a series of membranes with different mass fraction of TiNS were prepared. For both Li^+ and Mg^{2+}, the permeation rates dropped with increasing mass fraction of TiNS, suggesting that TiNS will hinder the permeation of ions.

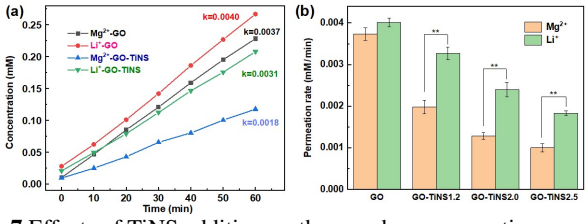

Fig. 7 Effects of TiNS addition on the membrane separation performance of mono-/di-valent ions. (a) Changes of ion concentration with time; (b) Changes of ion permeation rate with different mass fraction of TiNS.

As indicated in Figure 7b, the permeation rate of Mg^{2+} decreased faster than that of Li^+. Therefore, we calculated the Li^+/Mg^{2+} separation ratio of the membranes, which is 1.08, 1.65, 1.87, and 1.83 for GO, GO-TiMS1.2, GO-TiNS2.0, and GO-TiNS2.5 membranes (Table 1), respectively. Our results indicate that TiNS could increase the separation capability of

the GO membrane between Li^+ and Mg^{2+}. The best selectivity was achieved with 2.0% of TiNS in GO.

Table 1 Li^+/Mg^{2+} selectivity of the membranes prepared from GO-TiNS and previously reported membranes.

Membrane	Ion Separation Ratio (Li^+/Mg^{2+})	Reference
GO	1.08	This work
GO-TiNS1.2	1.65	This work
GO-TiNS2.0	1.87	This work
GO-TiNS2.5	1.83	This work
Nitrate ZnAl-LDH	Up to 6	25
GO	1.25	26
Ti_3C_2Tx	8.75	26
PIP-WCNTs/PEI/PES	7	27
DAPP/TMC	∼3	28
UiO-66-COOH	200	29
COF ($TpBDMe_2$)	217	28

Discussion

Ion selectivity is a highly desired property of membrane technologies for water purification, isolation and recovery of valuable resources from industrial water[1]. As lithium demand increases for applications like batteries, it is essential for efficient lithium extraction, particularly from brines, which is a significant challenge in the field of water treatment and resource recovery. Therefore, the development of new, energy-efficient separation techniques, especially for Li/Mg separation, is urgently required.

Membranes made from 2D materials have demonstrated excellent potential in the field of ion separation[6], such as graphene, GO, MXenes, metal organic frameworks (MOFs) and covalent organic frameworks (COFs). The tunable microstructures and multifunctional reactive groups offer GO membranes great potential in water desalination and gas purification[6]. However, the variable size of the interlayer spacing between GO sheets and the tendency of GO membranes to swell in aqueous solution, greatly affect the applications of GO membranes. Modulating the interlayer channel of GO membrane by building multilayer architectures has been proven to be effective to enhance ion selectivity. For example, a multilayer membrane was constructed based on graphene and sulfonated anino-polystyrene (rGO@SAPS) for selective separation of lithium ions[23].

Exfoliation of layered 2D materials would provide rich source of nanosheets for constructing layered membranes. Various exfoliation methods have been developed recently, such as mechanical, hydrothermal, electrochemical, and laser/microwave-assisted exfoliation methods[24]. The most commonly used method is liquid-phase exfoliation. In this study, the suspension of few-layer titanate nanosheets of about 2.3 nm in thickness and 1 2 μm in lateral size was exfoliated from titanate crystals via intercalation of TMBOH. Unilamellar GO were commercially obtained of 0.8-1.2 nm in thickness and 50-200 nm in lateral size. With monolayer sheets of GO and TiNS, we fabricated the composite membrane by vacuum filtration of aqueous solution without using any organic solvent, which is environmentally friendly. The membrane selectivity of Li^+/Mg^{2+} increased with the increasing mass fraction of TiNS, suggesting that TiNS promotes compact stacking of GO nanosheets, resulting in improved layer alignment.

By adding a small amount of TiNS nanosheets, the ion selectivity of the GO membrane was significantly improved. The Li^+/Mg^{2+} separation ratio of GO-TiNS membrane was compared with representative membranes reported previously, including micro-sized nitrate ZnAl LDH membranes, MXene-based membranes, covalent organic frameworks (COFs) membranes and metal-organic frameworks (MOFs) membranes (Table 1)[25–30]. However, the Li^+/Mg^{2+} selectivity of GO-TiNS is the lowest value, which is two orders of magnitude lower than the COF membranes. Nevertheless, our approach offers a novel pathway for enhancing ion selectivity through the strategic integration of titania.

Differential separation of ions depending on both the hydration radius and charge of the ions. Layered membranes can be controlled by changing flake size, interlayer distance and membrane thickness. Sun et al.[31] compared the ion penetration properties of GO membranes prepared from nanosize and microsize GO sheets, respectively. They demonstrate that nano-GO membranes have few wrinkles on the surfaces, while the surfaces of micro-GO membranes were corrugated, resulting in significantly increased permeability of all the cations in nano-GO membranes compared to micro-GO membranes. The interlayer distance of GO sheets can be modulated by inserting large chemical groups, soft polymer chains or even larger-sized nanoparticles[25]. Material load can also impact the desalination performance of GO membranes[32]. By adjusting the mass fraction of TiNS, the selectivity of the GO-TiNS composite membrane was potentially enhanced. However, cross-sectional SEM observation revealed that the layered structure was not densely compact (Figure 5d), probably because of the lateral microsize of TiNS sheets, which potentially reduced the membrane performance. To enhance the selectivity of the GO-TiNS composite membrane, improvements in the membrane structure are essential.

The permeation of salts seems to be controlled by surface charge of membranes. By tuning the membrane surface charge from highly positive to highly negative, $MgCl_2$ permeability continuously increased while Na_2SO_4 permeability showed a linear reduction[9]. The charge state of TiNS depends on the surface pH. At low pH, the nanosheets are positively charged, while at high pH, they are negatively charged[33]. Therefore, the ion separation of GO-TiNS membranes may be modulated with pH adjust. Future research is needed to fundamentally

understand the potential separation mechanism in the composite membrane, and thus to improve the ion selectivity.

Conclusion

In this study, we successfully synthesized titania nanosheets (TiNS) from potassium lithium titanate single crystals through acid-exchange and exfoliation methods. The characteristics of the resulting crystallites were thoroughly examined using SEM, TEM, and AFM, confirming the presence of monolayer sheets within the colloidal solution. We then fabricated composite membranes composed of GO and TiNS via vacuum filtration of a well-dispersed mixture of GO nanosheets and a specific mass ratio of TiNS. The ion selectivity of these membranes was assessed, revealing that the incorporation of TiNS reduced the membrane's permeation capacity while enhancing Li^+/Mg^{2+} separation. Although the separation performance of this work did not reach the best level, this preliminary work demonstrates the potential of GO-TiNS composite membranes in the area of membrane separations. Future work will be needed to enhance the separation performance, and systematically assess the membrane's performance against other ions, under varying pH, temperature, and long-term stability.

Methods

Synthesis of Titania Nanosheets

TiNS was synthesized using the protocol reported previously[7]. Typically, chemicals of K_2CO_3, TiO_2, and Li_2CO_3 were mixed intimately in a molar ratio of 10.4:2.4:0.8 and reacted at 900 °C for 20 h. The crystal of $K_{0.8}Ti_{1.73}Li_{0.27}O_4$ was obtained and subsequently converted into $H_{1.07}Ti_{1.73}O_4$ in 0.5 mol/L of HCl solution by stirring for 3 days. To produce single-layer TiNS dispersion, protonic titanate crystals were delaminated in tetrabutylammonium hydroxide ($(C_4H_9)_4NOH$; TBAOH) solution for 7 days with a solid-to-solution ratio of 4 mg/mL.

Fabrication of GO-TiNS Membranes

Graphene Oxide nanosheet aqueous suspension (XF020, 2 mg/mL, diameter: 50–200 nm) was purchased from Nanjing XFNANO Technology Co., Ltd., China. The GO-TiNS composite membranes were prepared through vacuum filtration of a homogeneously dispersed mixture of GO nanosheets and TiNS. A diluted GO suspension was mixed with TiNS for 20 min by sonication followed by stirring at 500 rpm for 3 h to obtain a homogeneous dispersion. The GO-TiNS dispersion was filtered through a hydrophilic PVDF membrane (0.45 μm pore size). Samples were prepared with different mass fractions of TiNS at 0, 1.2, 2.0, and 2.5 wt%, respectively. The resulting membranes were dried at 40 °C for 12 h.

Ion Permeation Test

A side-by-side H-cell was used to evaluate the membrane performance. DI water was added as the raw liquid, and 0.1 M salt solution ($MgCl_2$ or LiCl) was used as the draw solution. The membrane was placed between two compartments and faced the draw solution. The two compartment cells were stirred simultaneously during the test. After testing, DI water was used to soak for 2 h to clean the membrane. The test was carried out at room temperature. The ion permeation rate J (mM/min) was calculated using the following equation:

$$J = \frac{C_t - C_0}{t},$$

where C_0 (mM) and V_0 (L) represent the initial salt concentration and solution volume on the raw side, respectively. C_t (mM) and V_t (L) are the salt concentration and solution volume after running for a given time, and t (min) is the operating time. The conductivity of the solution on the raw side was measured by a conductivity meter (DDS 307A, Shanghai INESA Scientific Instrument Co., Ltd) to determine changes in salt concentration. The membrane selectivity, defined as the separation ratio, was calculated by the following equation:

$$S = \frac{J_{\mathrm{Li}}}{J_{\mathrm{Mg}}},$$

where J_{Li} and J_{Mg} represent the mean permeation rates of Li^+ and Mg^{2+} through a membrane, respectively.

Characterization

A scanning electron microscope (SEM, Zeiss Gemini 500, Germany) was used to study the morphology of the produced titania crystals. The XRD patterns were recorded using a Rigaku Miniflex-600 operated at 40 kV voltage and 15 mA current with Cu Kα radiation ($\lambda = 0.15406$ nm) at a step width of 5° min^{-1}. The obtained titania nanosheets were characterized for their lateral dimensions and thickness using a Hitachi HT7700 transmission electron microscope (TEM) and a Bruker Multimode 8 atomic force microscope (operated in PeakForce Tapping mode). The top-view and cross-sectional microstructure of membrane samples were examined using an SEM (QUANTA FEG 250, United States) at an accelerating voltage of 5–10 kV. The membranes were also inspected using an attenuated total reflectance Fourier transform infrared spectrometer (ATR-FTIR, Nicolet iN10, Thermo Scientific) by scanning from 4000 to 400 cm^{-1} at 2 cm^{-1} resolution.

Acknowledgements

I would like to express my gratitude to Dr. Yanfang Guan from the University of Science and Technology of China for her

continued guidance and support in my research every step of the way. I would also like to thank the staff at the University Testing Center for their patience in assisting me with sample characterization.

References

1 R. Sujanani, M. Landsman, S. Jiao, J. Moon, M. Shell, D. Lawler, L. Katz and B. Freeman, *Designing solute-tailored selectivity in membranes: perspectives for water reuse and resource recovery*.

2 S. Asensio-Delgado, F. Pardo, G. Zarca and A. Urtiaga, *Absorption separation of fluorinated refrigerant gases with ionic liquids: Equilibrium, mass transport, and process design*.

3 I.-D. Gerbaud, L. Hegely, P. Lang, F. Denes and X. You, *Review of extractive distillation. Process design, operation, optimization and control*.

4 L. Cisternas, C. Vásquez and R. Swaney, *.On the design of crystallization-based separation processes: Review and extension*.

5 R. Epsztein, R. DuChanois, C. Ritt, A. Noy and M. Elimelech, *Towards single-species selectivity of membranes with subnanometre pores*.

6 P. Liu, J. Hou, Y. Zhang, L. Li, X. Lu and Z. Tang, *Two-dimensional material membranes for critical separations*, https://doi.org/10.1039/d0qi00307g.

7 D. Lu, Z. Yao, L. Jiao, M. Waheed, Z. Sun and L. Zhang, *Separation mechanism, selectivity enhancement strategies and advanced materials for mono-/multivalent ion-selective nanofiltration membrane*.

8 Z. Wang, C. Ma, C. Xu, S. Sinquefield, M. Shofner and S. Nair, *Graphene oxide nanofiltration membranes for desalination under realistic conditions*.

9 M. Zhang, K. Guan, Y. Ji, G. Liu, W. Jin and N. Xu, *Controllable ion transport by surface-charged graphene oxide membrane*.

10 Y. Zhao, W. Shi, B. Bruggen, C. Gao and J. Shen, *Tunable nanoscale interlayer of graphene with symmetrical polyelectrolyte multilayer architecture for lithium extraction*.

11 M. Ohwada, K. Kimoto, T. Mizoguchi, Y. Ebina and T. Sasaki, *Atomic structure of titania nanosheet with vacancies*.

12 J. Hou, Y. Zheng, Y. Su, W. Zhang, T. Hoshide, F. Xia, J. Jie, Q. Li, Z. Zhao, R. Ma, T. Sasaki and F. Geng, *Macroscopic and strong ribbons of functionality-rich metal oxides from highly ordered assembly of unilamellar sheets*.

13 W. Qian, H. Fu, Y. Sun, Z. Wang, H. Wu, Z. Kou, B. Li, D. He and C. Nan, *Scalable assembly of high-quality graphene films via electrostatic-repulsion aligning*.

14 P. Sun, M. Zhu, R. Ma, K. Wang, J. Wei, D. Wu, T. Sasaki and H. Zhu, *Graphene oxide/titania hybrid films with dual-UV-responsive surfaces of tunable wettability*.

15 A. Volkov, S. Paula and D. Deamer, *Two mechanisms of permeation of small neutral molecules and hydrated ions across phospholipid bilayers*.

16 A. Waheed, U. Baig and I. Aljundi, *Fabrication of polyamide thin film composite membranes using aliphatic tetra-amines and terephthaloyl chloride crosslinker for organic solvent nanofiltration*.

17 H. Kaur, B. Rana, D. Tomar, S. Kaur and K. Jena, *Modern Techniques of Spectroscopy, Springer Nature Singapore*, vol. 17, p. 17.

18 H. Zhang, X. Wang, N. Li, J. Xia, Q. Meng, J. Ding and J. Lu, *Synthesis and characterization of TiO2/graphene oxide nanocomposites for photoreduction of heavy metal ions in reverse osmosis concentrate*.

19 A. Nasir, S. Khalid, T. Yasin and A. Mazare, *A review on the progress and future of TiO2/graphene photocatalysts*.

20 M. Gonzalez, J. Rieumont, F. Figueras and P. Quintana, *Drug–matrix interactions in nanostructured materials containing fluoxetine using sol-gel titanium oxide as a matrix*.

21 Z. Zhang, H. Schniepp and D. Adamson, *Characterization of graphene oxide: Variations in reported approaches*.

22 Q. Huang, S. Liu, Y. Guo, G. Liu and W. Jin, *Separation of mono-/di-valent ions via charged interlayer channels of graphene oxide membranes*.

23 Y. Zhao, C. Zhou, J. Wang, H. Liu, Y. Xu, J. Seo, J. Shen, C. Gao and B. Bruggen, *Formation of morphologically confined nanospaces via self-assembly of graphene and nanospheres for selective separation of lithium*.

24 W. Zheng and L. Lee, *Beyond sonication: Advanced exfoliation methods for scalable production of 2D materials*.

25 B. Li, J. Peng, M. Li, Z. Yang, J. Lu and J. Han, *Facile synthesis and exfoliation of micro-sized LDH to fabricate 2D membranes towards Mg/Li separation*.

26 C. Ren, K. Hatzell, M. Alhabeb, Z. Ling, K. Mahmoud and Y. Gogotsi, *Charge- and size-selective ion sieving through Ti3C2Tx MXene membranes*.

27 H. Zhang, Z. Xu, H. Ding and Y. Tang, *Positively charged capillary nanofiltration membrane with high rejection for Mg2+ and Ca2+ and good separation for Mg2+ and Li+*.

28 X. Li, C. Zhang, S. Zhang, J. Li, B. He and Z. Cui, *Preparation and characterization of positively charged polyamide composite nanofiltration hollow fiber membrane for lithium and magnesium separation*.

29 J. Lu, H. Zhang, X. Hu, B. Qian, J. Hou, L. Han, Y. Zhu, C. Sun, L. Jiang and H. Wang, *Ultraselective monovalent metal ion conduction in a three-dimensional sub-1 nm nanofluidic device constructed by metal–organic frameworks*.

30 F. Sheng, B. Wu, X. Li, T. Xu, M. Shehzad, X. Wang, L. Ge, H. Wang and T. Xu, *Efficient ion sieving in covalent organic framework membranes with sub-2-nanometer channels*.

31 P. Sun, F. Zheng, M. Zhu, Z. Song, K. Wang, M. Zhong, D. Wu, R. Little, Z. Xu and H. Zhu, *Selective trans-membrane transport of alkali and alkaline earth cations through graphene oxide membranes based on cation-interactions*.

32 W. Li, W. Wu and Z. Li, *Controlling interlayer spacing of graphene oxide membranes by external pressure regulation*.

33 S. Sáringer, P. Rouster and I. Szilágyi, *Regulation of the stability of titania nanosheet dispersions with oppositely and like-charged polyelectrolytes*.